Journal of Analytical and Applied Pyrolysis, Volume 149, August 2020, Article number 104831
DOI:10.1016/j.jaap.2020.104831

Hydrochloric acid removal from the thermogravimetric pyrolysis of PVC

D. Torres [a*], Y. Jiang [a], D.A. Sanchez Monsalve [b], G.A. Leeke [a,c]

[a] *Centre for Thermal Energy Systems and Materials, School of Water, Energy and Environment, Cranfield University, Cranfield MK43 0AL, UK*

[b] *Recycling Technologies Ltd, Swindon SN3 4TQ, UK*

[c] *School of Chemical Engineering, University of Birmingham B15 2TT, UK*

Abstract:

A powder characterization method was developed to screen the ability of a range of chemicals and absorbents to retain chlorine from chlorinated plastic pyrolysis. The behaviour of adsorbents such as Al_2O_3 and zeolites, and chemical removers based on $NaHCO_3$, CaO and Na_2CO_3-ZnO were studied for the removal of HCl released during PVC pyrolysis. First, chlorine removers are mixed with PVC and tested in a thermobalance under pyrolysis conditions for the complete PVC dehydrochlorination (550 ºC). Subsequently, after the release of HCl, CO_2 and H_2O, the chars are analysed by FTIR, CHN elemental analysis and ESEM-EDS to determine the retention of chlorine on the chlorine removers. According to FTIR and CHN, PVC pyrolysis occurs through dehydrochlorination and the formation of aromatics. FTIR and EDS were used to follow the consumption of the bases present in the chemical removers and the suppression of the C–Cl absorption bands of the PVC –CHCl– groups during pyrolysis, as well as the formation of the resulting salts (NaCl, $CaCl_2$ and $ZnCl_2$). The chemical removers exhibited chlorine retentions of up to 71 wt. % (using Na_2CO_3-ZnO), while the adsorbents presented a maximum of 19 % of retention at 550 ºC and heating rate of 200 ºC/min.

* Corresponding author. E-mail address: Daniel.Torres-Gamarra@cranfield.ac.uk / dtorres@icb.csic.es (D. Torres).

Keywords: *chlorine removal; PVC dehydrochlorination; PVC pyrolysis; hydrochloric acid removers; thermogravimetric analysis; FTIR*

Highlights

- The behaviour of different HCl-removing materials in PVC pyrolysis is studied
- A powder characterization method to exam chlorinated plastic pyrolysis is developed
- FTIR shows the reactive species use and the PVC C–Cl absorption bands suppression
- EDS and FTIR confirm the chlorine salts formed (NaCl, $CaCl_2$ and $ZnCl_2$) in the chars
- Na_2CO_3-ZnO-based removers exhibited Cl retentions of up to 71 wt.% after pyrolysis

1 INTRODUCTION

Plastics use, and their growing global demand, is leading to the depletion of non-renewable fossil feedstocks. The lack of readily available suitable recycling methods is also leading to the accumulation of plastic waste causing significant environmental issues [1]. Plastic pyrolysis is gaining interest as an attractive method of recovering chemicals from plastic waste through a process known as feedstock recycling. Pyrolysis can utilise "dirty" plastics which cannot be recycled satisfactorily by other methods such as mechanical recycling. The pyrolysis of mixed waste plastics generates an oil with a high calorific value that is transportable and stored. However, the pyrolysis of waste containing PVC is still a challenge due to the generation of HCl which corrodes equipment and contaminates the products with organochlorine compounds [2,3]. The thermal decomposition of PVC has been extensively investigated [2-4], and a number of methods explored to generate a product with reduced chlorine content. These include preheating to dechlorinate the plastic waste, the dehydrochlorination of municipal plastic waste containing PVC, or the use of absorbents to capture the HCl generated in-situ [4-7]. Similarly, catalytic, stepwise pyrolysis or hydrothermal carbonization have also been implemented with this same objective [6,8-11].

In terms of practicality, the co-pyrolysis of PVC, in the presence of other plastics (PE, PP, PS or PET [12]) or biomass [13], has been investigated with an aim to reduce costs, enhance the pyrolysis of its components, or even dilute the chlorine products obtained [4,14]. In single-step co-pyrolysis, interactions of PVC with other hydrocarbon materials can generate new chlorinated compounds in addition to those from the PVC [4]. These interactions between different kinds of plastics were studied by many authors to establish their kinetics [15,16].

In stepwise pyrolysis, a dehydrochlorination step at temperatures below 350 ºC is either carried out before the pyrolysis at high temperature (up to 800 ºC) or involves the use of catalysts [7-9,17-19]. Up to 85-95 wt. % of the initial chlorine is removed in the first step avoiding high

temperature and pressure or the necessity of catalysts [8,20]. In this case, the co-pyrolysis comprising PS and polyolefinic plastics [8,12] or biomass [13] did not affect the PVC dehydrochlorination. In addition, hemicellulose is a sustainable chlorine adsorbent that has shown to reduce the HCl emissions when lignocellulose is included in the PVC pyrolysis [19], but can lead to a high acidic oil.

Catalysts or catalytic adsorbents in the pyrolysis of PVC or chlorinated waste have been employed. These include solid catalysts such as zeolites, FCC, mesoporous silica, $Al(OH)_3$, MoO_3, Al-Zn composite, Ni-, Ca- and iron oxide-based catalysts which have shown to reduce chlorine content in the liquid products [10,14,17,18,20-28]. If the dechlorination of the pyrolysis oil is considered, catalytic or high-pressure hydrogenation routes simultaneously deal with condensed HCl and organochlorine compounds [5,29]. On the other hand, dry scrubbing of pyrolysis exhaust gases or the use of hot filters and additives (in or ex-situ) are also alternatives explored for HCl conversion and the upgrading (quality or distribution) of the pyrolysis products. Those investigated include Ca-based adsorbents ($Ca(OH)_2$, CaO, $CaCO_3$, lime), Na-based adsorbents ($NaHCO_3$, Na_2CO_3), metal oxides (MgO, Al_2O_3, SiO_2, PbO, ZnO, FeO, Fe_2O_3, red mud) and lanthanide oxides (La_2O_3, Nd_2O_3, CeO_2) [7,9,13,17,23,24,27,29-42]. In this work, a comprehensive powder characterization method was developed to screen the ability of a range of chemicals and absorbents to retain chlorine from the pyrolysis of chlorinated plastics. The behaviour of six different materials for the removal of hydrochloric acid released during the PVC pyrolysis was studied. Solid chlorine removers, including different adsorbents and chlorine scrubbers, were mixed with PVC (1:1; wt./wt.) and pyrolyzed in a thermobalance at 550 ºC until complete dehydrochlorination of PVC occurred. The resulting chars were analysed by Fourier transform infrared spectroscopy (FTIR), CHN elemental analysis and scanning electron microscopy-energy dispersive X-ray spectroscopy (ESEM-EDS). This is the first time that solid characterization techniques (TGA, FTIR and

ESEM-EDS) are used in a complementary way to compare the behaviour offered by the materials in the PVC dehydrochlorination process. Conventionally, the HCl present in the evolved gases released during the pyrolysis is measured by coupled TGA-spectroscopic techniques, such as FTIR. This new procedure is presented as a practical method, consuming just milligrams of the sample, to screen the ability of materials for use as HCl removers in the pyrolysis of PVC.

2 MATERIALS AND METHODS

2.1 Materials

Pure polyvinyl chloride, without additives or plasticisers, (Sigma Aldrich, purity > 99 %) was used as received. Two classes of chlorine removers were characterized and used. The first class were three chemical removers (that involved a chemical reaction during the process) based on $NaHCO_3$, CaO and Na_2CO_3-ZnO, and the second class were three adsorbents based on Al_2O_3 and NaX zeolites. Table 1 lists the elemental composition of these materials, which are labelled as Chem-$NaHCO_3$, Chem-CaO, Chem-Na_2CO_3-ZnO, Ads-Al_2O_3-1, Ads-Al_2O_3-2 and Ads-NaX. Chem-$NaHCO_3$ and Chem-CaO contain a low percentage of carbon as a dilutor of the active phase while Chem-Na_2CO_3-ZnO (1:1, wt./wt.) has a 30 wt. % SiO_2-Al_2O_3 as a support. Ads-Al_2O_3-1 and Ads-Al_2O_3-2 correspond to NaOH activated Al_2O_3 at low and high temperatures, respectively. In the case of mixtures, pure PVC and chlorine removers were physically mixed in a ratio of 1:1 (by weight).

Table 1 Elemental composition by EDS and CHN elemental analysis of chemical removers and adsorbents.

		Chem-$NaHCO_3$	Chem-CaO	Chem-Na_2CO_3-ZnO	Ads-Al_2O_3-1	Ads-Al_2O_3-2	Ads-NaX
EDS	**C**	20.05	9.90	2.19	0.00	0.00	0.00
(wt. %)	**O**	53.29	26.03	37.47	50.51	50.01	56.72

	Na	24.33	0.00	8.37	5.22	5.16	11.61
	Ca	0.00	63.52	0.60	0.00	0.00	0.29
	Al	0.96	0.00	7.70	41.58	40.98	12.99
	Zn	0.00	0.00	38.30	0.00	0.00	0.00
	Si	0.00	0.00	2.17	0.00	0.00	16.69
	Mg	0.00	0.00	0.83	0.00	0.00	0.83
	Fe	0.00	0.00	0.31	0.00	0.00	0.39
	Others	1.38	0.55	2.07	2.70	3.85	0.48
	C	21.63	10.64	4.19	1.21	1.66	0.20
CHN	**H**	1.25	2.37	1.13	1.66	1.74	2.59
(wt. %)	**N**	0.08	0.09	0.00	0.00	0.01	0.01
	Others	77.04	86.90	94.68	97.13	96.59	97.20
	H_2O[a]	1.59	3.01	7.48	7.72	8.05	15.38

a = Estimated according to the EDS and CHN data considering the species present in each case.

2.2 Thermobalance tests

The samples were prepared by grinding in a pestle and mortar and mixed to give the desired compositions. Thermogravimetric analyses were carried out in a Perkin Elmer TGA 8000™ thermogravimetric analyser. TGA profiles were obtained from a sample amount of 20±5 mg and using 40 ml min^{-1} of N_2 as an inert atmosphere for pyrolysis. The temperature program consisted of rapid heating of the sample (20 or 200 ºC/min) from room temperature to 550 ºC and a stabilization stage at this temperature for 20 min. 3 repetitions were performed for each material or mixture to obtain reproducible results. An average mass loss curve ("Average" in the corresponding TGA and DTG figures) was produced by taking the weighted average of the mass loss of pure PVC and the chemical remover/absorbent materials as follows:

$$M_{Average\_T}\,(g) = (M_{PVC\_T} + M_{Remover\_T}) / 2 \qquad \textbf{Equation 1}$$

Where $M_{Average\_T}$ is the average mass at a temperature T, and M_{PVC_T} and $M_{Remover\_T}$ are the masses of PVC and the chlorine remover at that temperature T. For this calculation, the curves of mass evolution of the PVC and the remover were obtained separately.

116 **2.3 Characterization of thermobalance chars**

117 Morphological assessment of the thermobalance chars was performed by environmental
118 scanning electron microscopy (ESEM, FEI Philips XL30) by examining the surface using a
119 back-scattered electrons detector. Coupled to the ESEM, an EDS analyser (Oxford Instruments,
120 X-Max detector) was used to study the chemical composition of the samples. Additionally,
121 EDS accuracy was adjusted for an adequate elemental quantification by determination and
122 subtraction of the contribution of the conductive tab used, measurement of different large areas
123 (at least 5 from 400 to 10,000 μm^2) of each sample, correction with data of the CHN elemental
124 analysis and verification with standards of known composition.

125 The chlorine retention obtained by a remover in the PVC pyrolysis (*Cl retention*) was
126 calculated as the percentage of chlorine content loss between that calculated in the char and
127 that in the virgin PVC:

128 $$Cl\ retention\ (wt.\ \%) = (M_{Cl\_Char} / M_{Cl\_PVC}) \times 100 \qquad \textbf{Equation 2}$$

129 Where M_{Cl_PVC} and M_{Cl_Char} correspond to the masses of Cl in the PVC and the char,
130 respectively. Both Cl masses depend on the mass of mixture (PVC + chlorine remover) loaded
131 in the thermobalance.

132 The FTIR transmittance spectrum for each sample was determined using a SHIMADZU
133 IRTracer-100 spectrophotometer. The FTIR was set to measure transmittance between 500
134 cm^{-1} and 4000 cm^{-1}. The number of scans and scan resolution were set at 15 and 4 cm^{-1},
135 respectively.

136 CHN elemental analysis was performed using a Perkin-Elmer CHN Elemental Analyzer.
137 Samples were combusted at 900 ºC in an oxygen atmosphere and the combustion gases were
138 passed over a copper catalyst to remove excess O_2 and to reduce the NO_x to elemental nitrogen.
139 CO_2, H_2O and N_2 were subsequently separated by frontal chromatography and quantified by a

thermal conductivity detector (TCD). For this measurement, TGA chars were dried at 105 ºC for at least 2 h and 0.020 g packed in aluminium-foil capsules.

3 RESULTS

3.1 Pyrolysis of PVC

Initially, TGA and DTG of PVC (Figure 1) at different heating rates (slow = 20 ºC/min and fast = 200 ºC/min) were performed to see the main mass losses produced during the pyrolysis. As expected for PVC, two main mass losses were observed: the first loss (Zone I), starting at 250-260 ºC is attributed to the release of HCl and monoaromatics as a result of PVC thermal decomposition, and the second loss (Zone II), starting at 400-450 ºC, is due to the degradation of the remaining organic materials [4]. A char-like material remained after the pyrolysis process (7.1-8.7 wt. %). Although the mass loss attained at the end of Zone I (up to 66.2 wt. %) comprises the release of the total HCl content in PVC (58.4 wt. %) along with the release of mainly benzene and toluene among other aromatics [43], the presence of chlorine derivatives in the char cannot be entirely discounted. In addition to the aromatic hydrocarbons (such as benzene, toluene, naphthalene, o-xylene, etc.) released in Zone I [15], aromatics are generated in higher amounts in Zone II, where condensation and de-alkylation reactions take place [2]. On the other hand, chlorinated aromatic hydrocarbon (mainly chlorobenzene) evolution has been detected at higher temperatures (Zone II) [3].

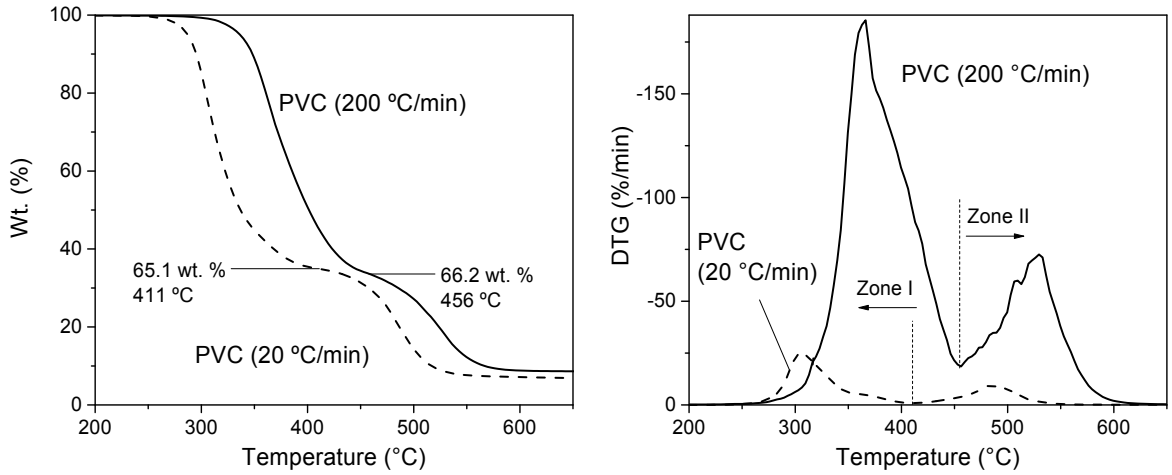

Figure 1 a) TGA and b) DTG profiles of pure PVC using N_2 at heating rates of 20 and 200 ºC/min.

At a heating rate of 200 ºC/min, the first mass loss ends when the temperature exceeds 450-480 ºC. The char generated was collected and analysed by FTIR (Figure 2) to see the chemical changes obtained in the char and to follow the variation in the C–Cl bond signals. Zhou et al. [44] showed that at 450 ºC, near-complete dehydrochlorination of the PVC is achieved, with a Cl content in the char typically below 1 wt. %.

The spectra of PVC before and after pyrolysis can give an idea of the dehydrochlorination mechanism [44,45]. The spectra shown in Figure 2 were similar to those previously reported for PVC and pyrolyzed PVC, and they were interpreted according to their assignments [44-50]. Despite these similarities (discussed below), both profiles showed differences in the intensities of some peaks concerning those reported, and their analysis serves as a starting point for when comparing the effectiveness of a chlorine remover. Adsorption bands above 2750 cm^{-1} in PVC and pyrolyzed PVC are due to C–H stretching vibration in –CH=CH– (3020 cm^{-1}), $–CH_2–$ (2846, 2855, 2911 and 2920 cm^{-1}) and –CHCl– (2816 and 2968 cm^{-1}) functional groups [44,46]. Bands associated with the –CHCl– groups disappeared clearly after pyrolysis, while those of –CH=CH– increased, clearly indicating that the dehydrochlorination generated C=C

bonds. Likewise, post pyrolysis, the bands associated with chlorine-free molecules were more prominent. For example, the methylene group peaks (–CH_2–) shifted from 2911 and 2846 cm^{-1} to 2920 and 2855 cm^{-1}, respectively [44]. These displacements would be motivated by the different nature of these functional groups: methylene in the original PVC and the aromatic network present in dehydrochlorinated PVC as a result of the transformation of conjugated double bonds [44]. Absorption bands in the range 1800-1000 cm^{-1} mainly correspond to vibrations of double bonds stretching and of C–H deformation. Pyrolyzed PVC presented a new large band at 1599 cm^{-1} which was assigned to C=C stretching in conjugated –C=C– bonds, for both aliphatic and aromatic compounds [47,48]. As in the case of the 2911 cm^{-1} band, the band at 1425 cm^{-1}, associated with the C–H bending in –CH_2– groups, shifted to 1441 cm^{-1} due to the formation of new methylene groups generated during the transformation of conjugated double bonds. Other bands present in the PVC spectrum such as those at 1198 cm^{-1} and 1094 cm^{-1}, associated with the C–H rocking in methylene groups and the PVC skeletal vibration (Cl–C–H), respectively, are not present after pyrolysis. Besides, the bands associated with the C–H bending in –CHCl– groups (at 1329 and 1254 cm^{-1}) also disappeared. Other bands at 959 and 833 cm^{-1} related to the C–H rocking of –CH_2– in PVC are not present after pyrolysis. Just as double C=C bonds are formed during the pyrolysis, the new bands at 870, 810, 745 and 700 cm^{-1} are attributed to aromatic products, specifically to the =C–H out of plane vibration in aromatic rings [47,48]. It has been shown that the intramolecular reactions of cyclization and aromatization start at temperatures around 300 ºC during PVC pyrolysis [44], although above 400 ºC Diels–Alder reactions between conjugated dienes and olefins on different chains could also occur [2].

The original structure of PVC is destroyed after its thermal dehydrochlorination and the char obtained after pyrolysis does not show the C–Cl stretching bands in its spectrum (at 685 and 606 cm^{-1}). The decrease in Cl for the sample pyrolyzed at 480 ºC reached 93 wt. % as shown

by the CHN elemental analysis (C = 90.51 wt. %; H = 5.39 wt. %; N = 0.09 wt. %; Difference = 4.02 wt. %). However, this value obtained by difference could imply the presence of other elements in addition to Cl such as O, which was found to be present at 1.9 wt. % by ESEM-EDS. Taking into account the O, the reduction of Cl obtained would be 96 wt. %. At temperatures above 450 ºC, the Cl content in the char has been reported to be below 1.05 wt.% [44]. According to FTIR and CHN analysis data, the PVC pyrolysis occurs through a clear dehydrochlorination process and the formation of aromatic compounds.

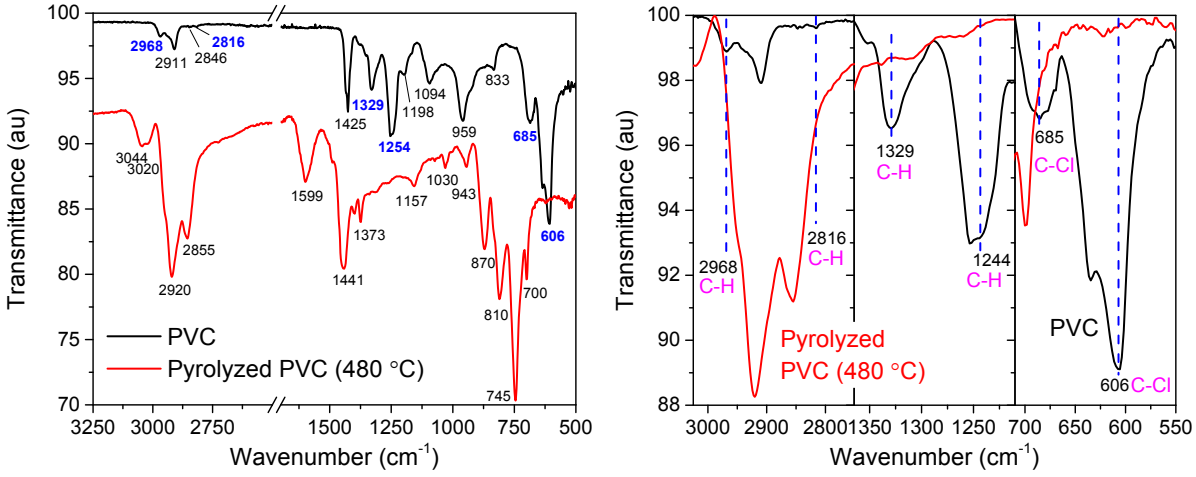

Figure 2 a) FTIR spectra of pure PVC and PVC pyrolyzed at 480 ºC. b) Zoom of the three zones of bands associated with C–H and C–Cl stretching in the –CHCl– groups (shown in blue in a)).

3.2 Chemical removers and adsorbents behaviour in the PVC pyrolysis

As a preliminary measurement of chlorine removal, the use of chemical removers and adsorbents were used and in conjunction with the PVC by undertaking pyrolysis in the thermobalance (Figure 3 and Figure 4). Pyrolysis was carried out in an N_2 stream up to 550 ºC (with a 20 min isothermal period). This temperature ensures the total dehydrochlorination of the original PVC. Chlorine removers were physically mixed with pure PVC (1:1; by weight).

Single materials gave mass losses around 10 wt. % for the studied heating rate (200 ºC/min), except for Chem-$NaHCO_3$ (33.1 % wt. loss). This loss was mainly in the 100-225 ºC range and mostly arises from the humidity trapped in the materials in accordance with the EDS and CHN elemental analysis results shown in Table 1. The higher mass loss shown by Chem-$NaHCO_3$ is due to the thermal decomposition of $NaHCO_3$ into Na_2CO_3, CO_2 and H_2O.

The presence of a chemical remover/adsorbent in the PVC pyrolysis promoted a measurable variation in the mass loss recorded in Zone I and at the end of the process (550 ºC), and suggests a possible indication of chloride retention. An average mass loss curve ("Average" in the figures) was produced by taking the weighted average of the mass loss of pure PVC and the chemical remover/absorbent materials. The difference between the mixed PVC-remover mass loss and the average curve could indicate a possible chemical reaction or physical adsorption of the HCl gas emitted during the pyrolysis process. Thus, the formation of salts with a molecular weight higher than those of their respective bases after the reaction is expected to be seen by this technique for the chemical removers (see in equations 3 to 5). The existence of a chemical reaction (or adsorption process) is more evident when looking at the Zone I of the DTG curves where the PVC dehydrochlorination process occurs. Table 2 summarises the differences in the mass losses for PVC mixed with the different chlorine removers. The compositions of the chemical removers $NaHCO_3$ (Chem-$NaHCO_3$), CaO (Chem-CaO), ZnO and Na_2CO_3 (Chem-Na_2CO_3-ZnO) can react with acidic HCl gas releasing H_2O only or H_2O and CO_2 depending on the base used as shown in equations 3 to 5 below. As mentioned before, $NaHCO_3$ in Chem-$NaHCO_3$ decomposes completely into Na_2CO_3 during the process. The formation of Na_2CO_3 is completed before the dehydrochlorination of PVC occurs, as is clearly seen in Figure 3, therefore, the reaction between $NaHCO_3$ and the released HCl does not take place (reaction not included in the equations shown below). The formed salts of $CaCl_2$, $ZnCl_2$

247 and NaCl will remain in the char after the pyrolysis, and change the final char mass when
248 compared to that of the average curve, as long as the chemical reaction occurs.
249 The reactions between the bases of the chemical removers and HCl gas [37,51-53] are given
250 as:
251 Chem-$NaHCO_3$ and Chem-Na_2CO_3-ZnO:
252 Na_2CO_3 (s) + 2HCl (g) → 2NaCl (s) + H_2O (g) + CO_2 (g); ΔH^0 = -142.2 kJ/mol **Equation 3**
253 Chem-CaO:
254 CaO (s) + 2HCl (g) → $CaCl_2$ (s) + H_2O (g); ΔH^0 = -217.9 kJ/mol **Equation 4**
255 Chem-Na_2CO_3-ZnO:
256 ZnO (s) + 2HCl (g) → $ZnCl_2$ (s) + H_2O (g); ΔH^0 = -124.3 kJ/mol **Equation 5**
257
258 Given the difference between the actual and average behaviour of the chlorine removers, some
259 parameters are of interest: the temperature at which dehydrochlorination begins (*onset*), the
260 temperature of the maximum gas release (T_{max}) and the mass loss after Zone I. These parameters
261 are included in Table 2. In all mixtures, the manifestation of a chemical reaction or an
262 adsorption process is noticeable due to the observable changes in Zone I, where smaller but
263 faster weight losses can be observed, which generates a distinguishable peak that concentrates
264 the main release of gas at a temperature (T_{max}), as well as the delay of the *onset*. The most
265 drastic changes occur with the use of chemical removers, Chem-$NaHCO_3$, Chem-CaO and
266 Chem-Na_2CO_3-ZnO, which concentrate the release of gas in Zone I at a temperature close to
267 that of the pyrolysis of PVC alone (372.9 ºC, see T_{max} in Table 2). According to the chemical
268 reactions that can take place, the use of chemical removers causes a release of H_2O and CO_2
269 produced from the formation of the corresponding chlorine salt. Note, with the use of Chem-
270 CaO the only emission from the reaction of its base is H_2O. The adsorbents showed different
271 behaviours, Ads-Al_2O_3-1 and Ads-Al_2O_3-2 gave a low release rate of gas (much lower than in

the case of chemical removers) at 360 and 358 ºC, respectively, while with the use of Ads-NaX this was delayed to 397.5 ºC. The chemical removers Chem-Na_2CO_3-ZnO and Chem-CaO gave mass differences of -25.5 % and -24.6 % concerning the theoretical behaviour (see *Diff.* in Table 2). Among these results, the low mass difference calculated for Chem-$NaHCO_3$ (-5.5 %) stands out, but has also given the highest gas release per mole of remover as seen in DTG (at 381.2 ºC). Parallel reactions with gases generated from the thermal decomposition of $NaHCO_3$ could be involved behind this result. Additionally, in all cases, the gas release is delayed (see *ΔT* in Table 2), which was greatest for the chemical removers and Ads-NaX.

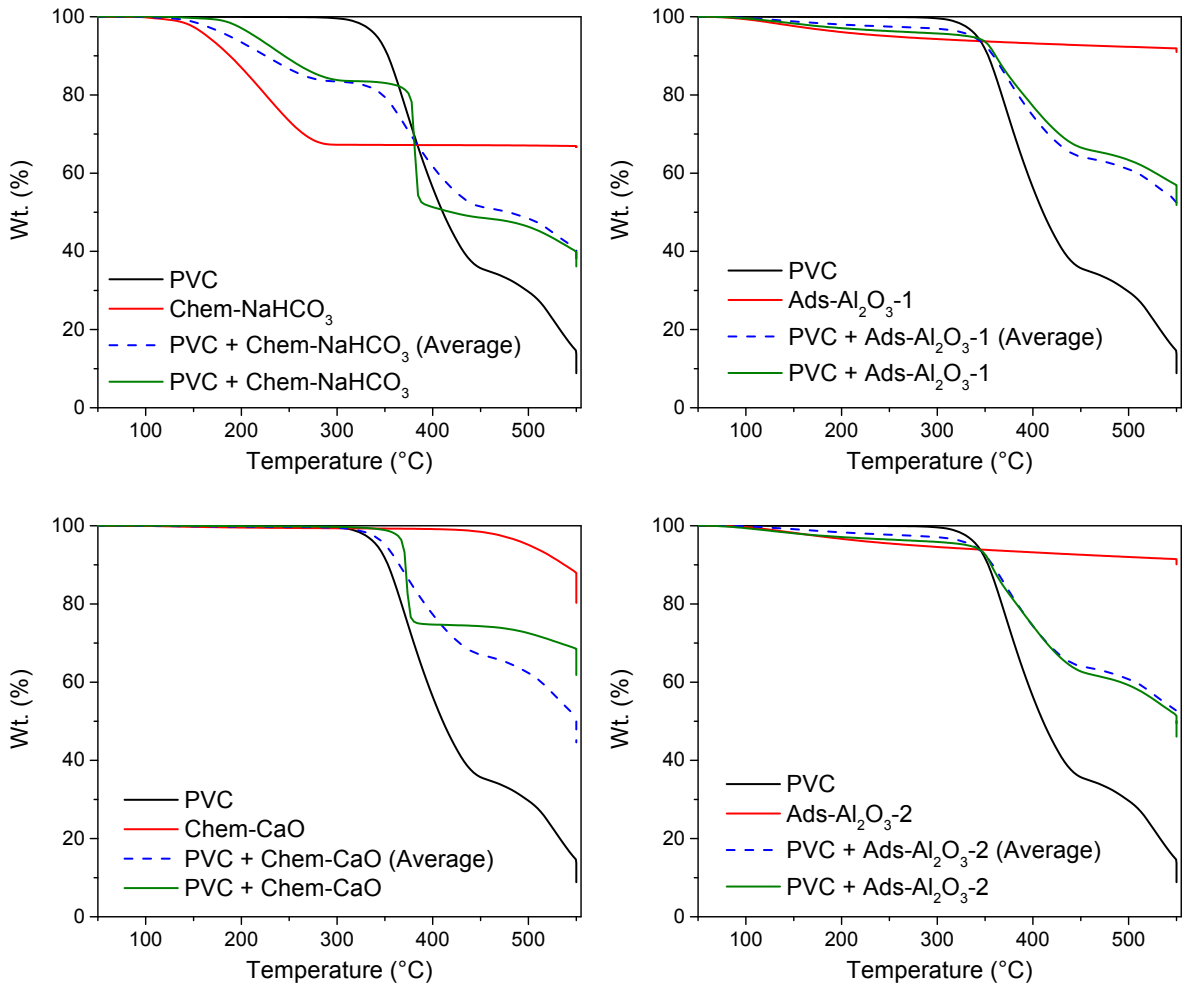

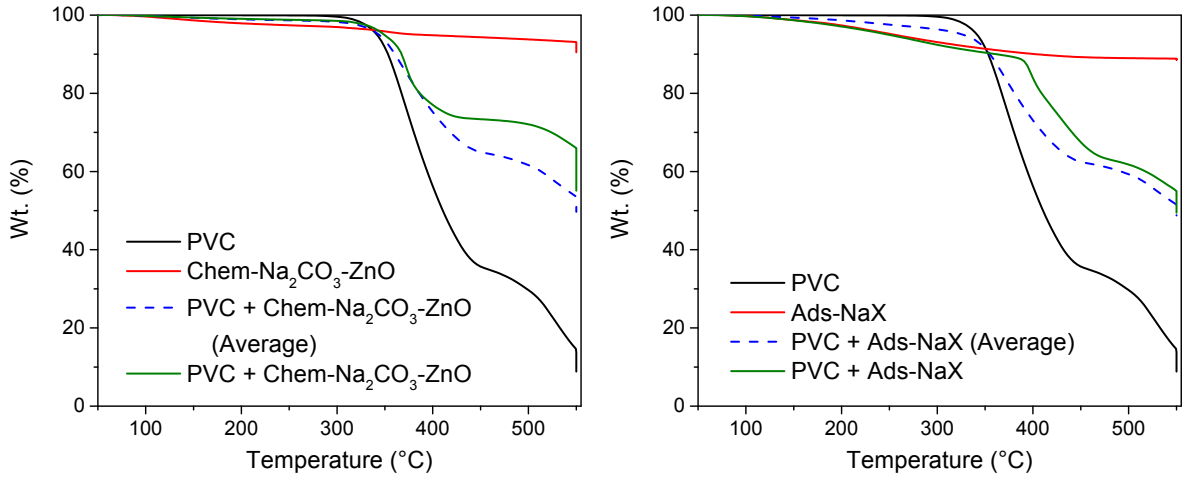

283

284 **Figure 3** TGA curves of PVC and additives (single and mixed). The average curve of the

285 mixture is also included. Heating rate of 200 ºC/min from room temperature to 550 ºC followed

286 by a hold of 20 min at this temperature.

287

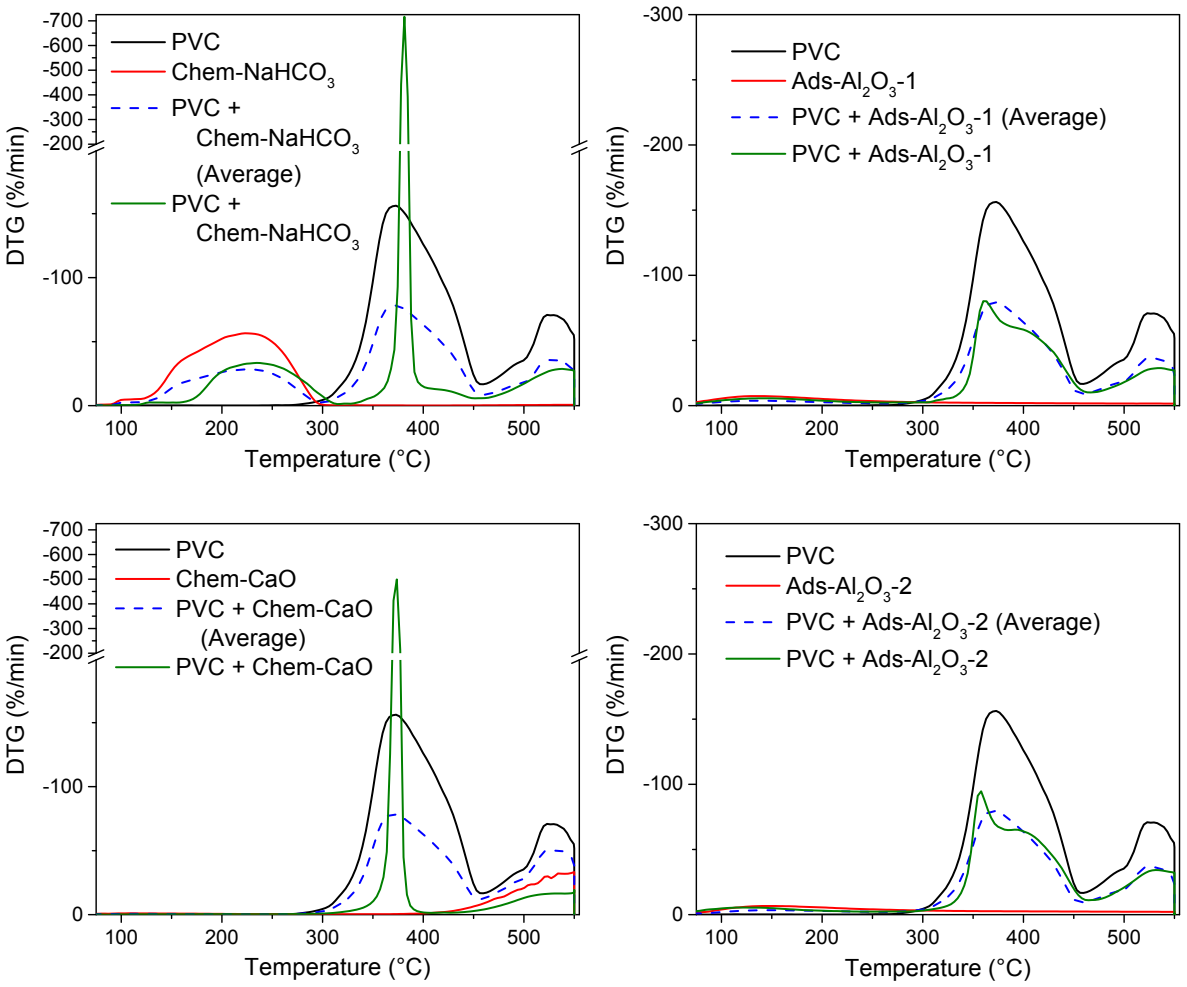

288

289

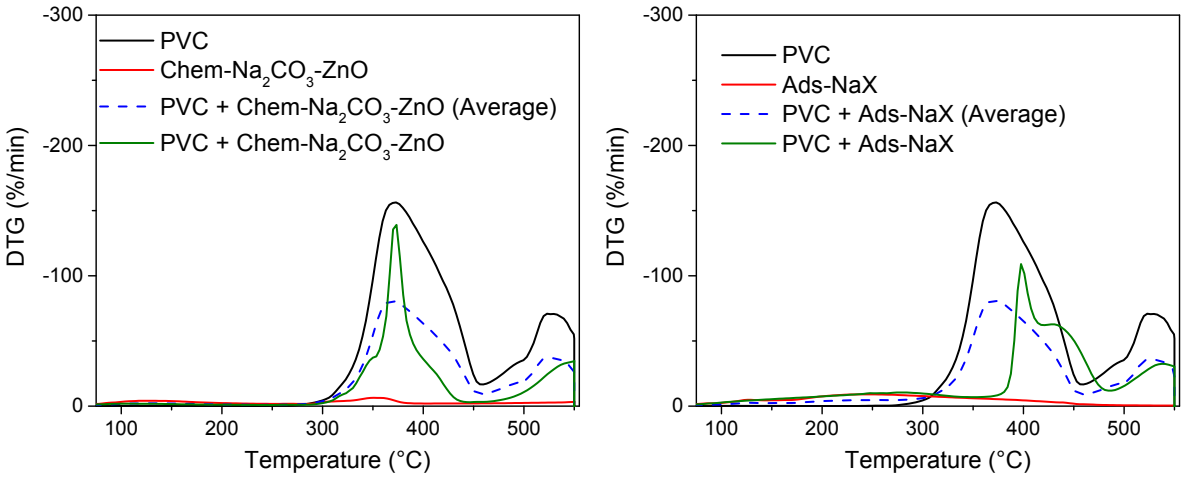

Figure 4 DTG curves of PVC and additives (single and mixed). The average curve of the mixture is also included. Heating rate of 200 ºC/min from room temperature to 550 ºC followed by a hold of 20 min at this temperature.

Table 2 Weight loss and *onset* data calculated from TGA and DTG curves of PVC and mixtures.

Sample	***Zone I*** *(wt. %)*	***Zone I*** [a] *(wt. %)*	***Diff.*** [b] *(%)*	T_{max} *(ºC)*	***Onset*** *(ºC)*	***Onset*** [a] *(ºC)*	ΔT [c] *(ºC)*
PVC	65.2	-	-	372.9	340.8	-	-
PVC + Chem-$NaHCO_3$	30.9	32.7	-5.5	381.2	399.6	342.2	57.4
PVC + Chem-CaO	25.1	33.3	-24.6	373.7	367.9	340.6	27.3
PVC + Chem-Na_2CO_3-ZnO	25.4	34.1	-25.5	373.3	357.0	338.5	18.5
PVC + Ads-Al_2O_3-1	30.6	33.7	-9.2	360.0	348.8	341.3	7.5
PVC + Ads-Al_2O_3-2	34.3	33.8	1.5	357.9	345.0	340.3	4.7
PVC + Ads-NaX	27.7	35.1	-21.1	397.5	390.5	341.9	48.6

a: Weight loss calculated from the average curve; b: Weight loss difference = (real weight loss - average weight loss) / average weight loss x 100; c: ΔT = Onset - Onset^a (a = average).

300 **3.3 Characterization of chars and measurement of chlorine retention**

301 As in the case of pure PVC (Figure 2), the chars generated from PVC/chlorine remover
302 mixtures after its pyrolysis at 550 ºC were analysed by FTIR to follow the changes in the signals
303 of the C–Cl and C–H bonds of the –CHCl– functional groups. The intention was to observe
304 whether dehydrochlorination of PVC is inhibited, as well as to identify bands of new groups
305 or salts including the Cl released during the process. Figure 5a-b and Figure 5c-d show the
306 FTIR spectra of chlorine removers and 1:1 mixtures, respectively, before and after pyrolysis at
307 550 ºC with a 20 min isothermal period. The main bands assigned to PVC and pyrolyzed PVC
308 in section 3.1 are included (as vertical lines) for comparison.

309 Chlorine removers showed components with very different contributions in the FTIR spectra
310 (see Figure 5a-b). The main bands presented for Chem-Na_2CO_3-ZnO, Chem-$NaHCO_3$ and
311 Chem-CaO correspond to the adsorption bands of Na_2CO_3, ZnO, γ-Al_2O_3 and SiO_2 [54-59],
312 $NaHCO_3$ [56], and CaO [60], respectively. No bands attributable to carbon were observed in
313 Chem-$NaHCO_3$ and Chem-CaO due to its low concentration (around 10 wt. %) and low
314 transmittance signal. On the other hand, adsorbents showed typical FTIR spectra of Al_2O_3
315 (Ads-Al_2O_3-1 and Ads-Al_2O_3-2) [59] and NaX zeolites (Ads-NaX) [61-63]. After pyrolysis in
316 the presence of the single chlorine removers, no significant changes in the FTIR spectra were
317 observed. For all cases, except Chem-$NaHCO_3$, in which the complete transformation of
318 $NaHCO_3$ into Na_2CO_3 is now confirmed, there was no change to their original FTIR spectra.
319 For Chem-Na_2CO_3-ZnO and Ads-NaX, a broad transmittance band associated with the
320 asymmetric stretching of Si–O–Si centred at the 930-990 cm^{-1} region stood out [63,64]. In the
321 case of Ads-NaX, this band includes the vibration of Si–O–Al bonds in found zeolites [64].

322 The 1:1 mixtures (see Figure 5c-d), shows the bands of the pure PVC and the chlorine remover
323 together: main FTIR bands of the PVC (discussed in Section 3.1) are noticeable in all mixtures.
324 However, significant changes in the FTIR spectra of the single materials have been observed

after the pyrolysis. At first inspection, the PVC C–Cl bond signals are notably absent post pyrolysis evidencing a complete dehydrochlorination of the PVC (see a zoom of the 775-500 cm^{-1} region in Figure 6). The chemical removers showed the disappearance of the bands relative to their bases (Na_2CO_3, ZnO, and CaO), which were present when they were pyrolyzed without the presence of PVC, and the formation of their respective chlorinated salts. Although all the chemical removers had an excess of base, only Chem-CaO showed the presence of the initial base that could still react with more HCl. Likewise, vibrations of the Ca–Cl and Zn–Cl bonds (marked in Figure 5c) from the $CaCl_2$ and $ZnCl_2$ salts were present in chars obtained when Chem-CaO and Chem-Na_2CO_3-ZnO were used in the PVC pyrolysis. Also, Chem-Na_2CO_3-ZnO presents a band around 610 cm^{-1} that could be associated with the Si–Cl bond vibration due to the formation of condensed $SiCl_4$ [65]. In the case of NaCl, despite observing the consumption of Na_2CO_3 in Chem-$NaHCO_3$ and Chem-Na_2CO_3-ZnO, its formation in FTIR profiles is imperceptible because this salt absorbs infrared light outside the 4000-500 cm^{-1} FTIR region. However, the presence of NaCl salt in the chars, as well as those of $CaCl_2$ and $ZnCl_2$, are confirmed by EDS (see explanation below). On the other hand, it is difficult to observe adsorption processes that may take place on the materials using FTIR, without considering that the pyrolysis temperatures could cause desorption of the HCl adsorbed during the process. In this regard, Al_2O_3 as adsorbent for HCl could desorb in the range 27-377 ºC [66]. Likewise, zeolites X showed good HCl adsorption at room temperature [67], resulting in its complete desorption at 450 ºC [68]. The transformation observed in the adsorbents is therefore minor and is mainly due to the thermal transformation of their constituents. However, Ads-NaX showed recognizable signals of PVC pyrolysis products, specifically those bands attributed to the =C–H vibration of aromatic compounds (at 870, 810, 745 and 700 cm^{-1}, [47,48]). Likewise, these bands are the most evident in the samples, mainly for Chem-$NaHCO_3$, Chem-Na_2CO_3-ZnO and Ads-NaX.

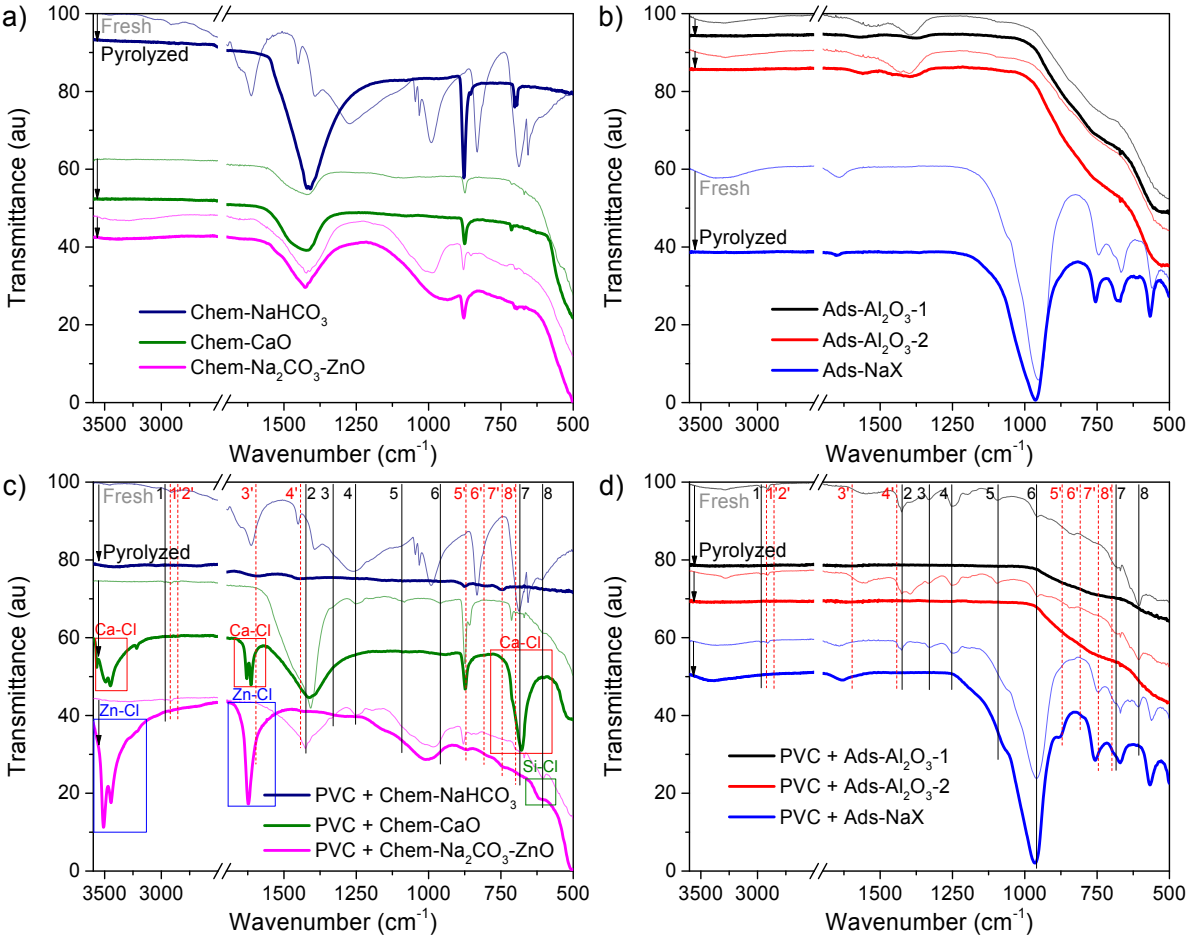

Figure 5*1* FTIR spectra of fresh and 550 ºC-pyrolyzed a) chemical removers and b) adsorbents, and FTIR spectra of mixtures of c) chemical removers and d) adsorbents with PVC. PVC Bands (black solid lines; data from Figure 2): 1 = 2968, 2 = 1425, 3 =1329, 4 = 1254, 5 = 1094, 6 = 959, 7 = 685 and 8 = 606 cm^{-1}. Pyrolyzed PVC Bands (red dashed lines; data from Figure 2): 1' = 2920, 2' = 2855, 3' = 1599, 4' = 1441, 5' = 870, 6' = 810, 7' = 745 and 8' = 700 cm^{-1}.

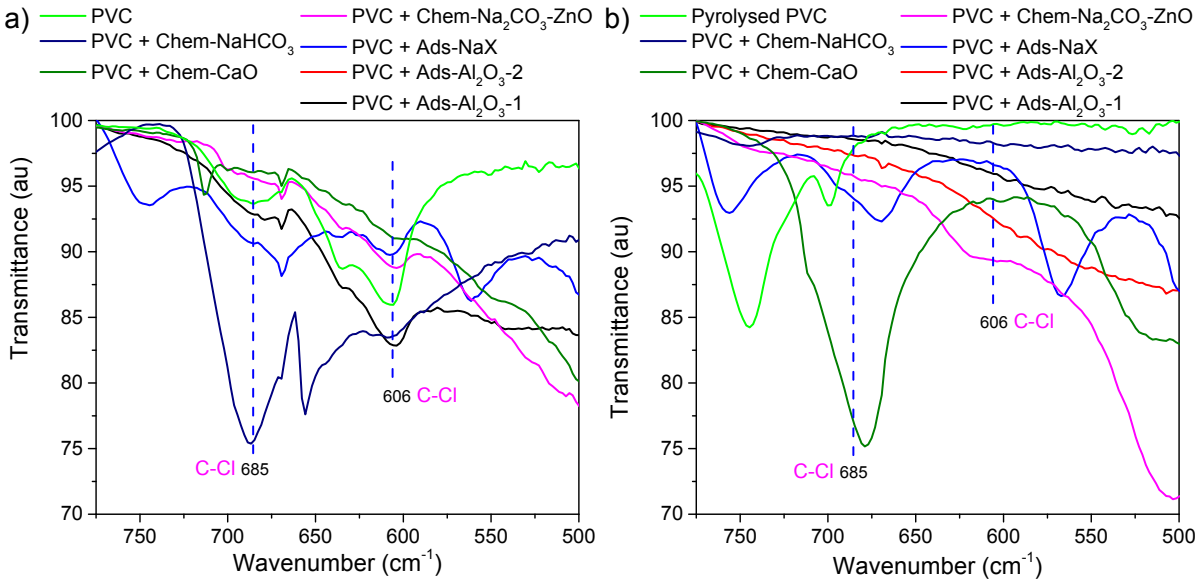

359

360 **Figure 6** Zoom of the FTIR 775-500 cm^{-1} region (from Figure 5c and Figure 5d) in a) fresh
361 and b) pyrolyzed mixtures. Dashed lines correspond to the theoretical position of the bands
362 associated with C–Cl stretching in the –CHCl– groups.

363

364 A morphological and chemical study of the chlorine removers before and after their use in the
365 PVC pyrolysis was undertaken by ESEM-EDS. Micrographs of starting materials can be found
366 in Figure 7. The carbon, easily distinguishable in the images of Chem-CaO and Chem-$NaHCO_3$
367 (Figure 7a and 7b), is completely separated from the bases. The image of Ads-NaX (Figure 7f)
368 stands out as it shows spheres of a few micrometres corresponding to NaX zeolites [61].

369

370 a)
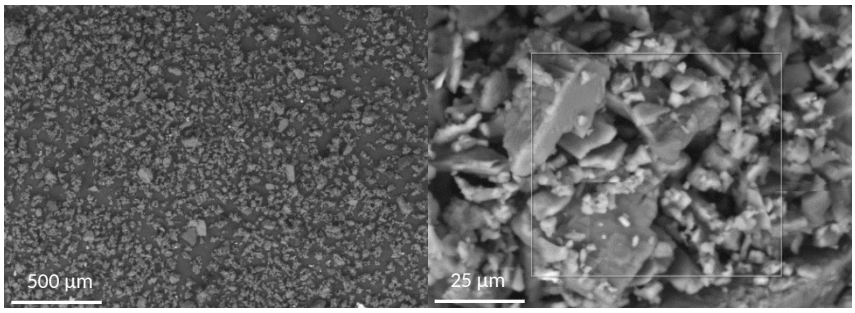

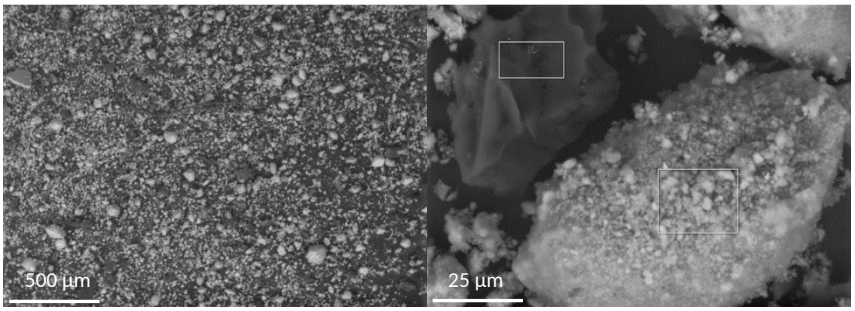

b)

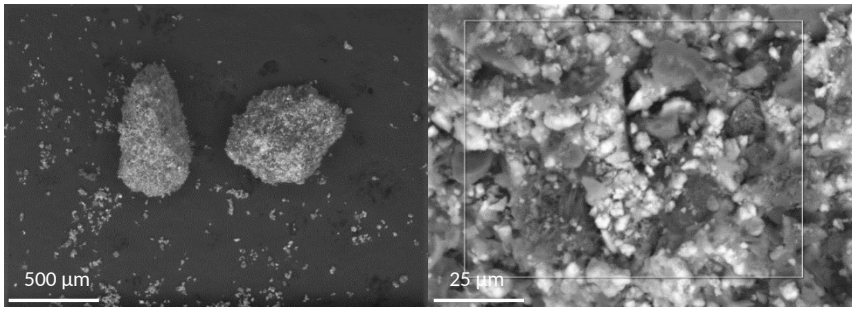

c)

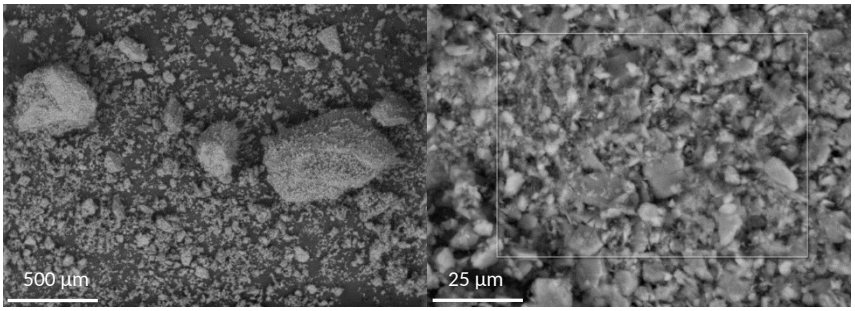

d)

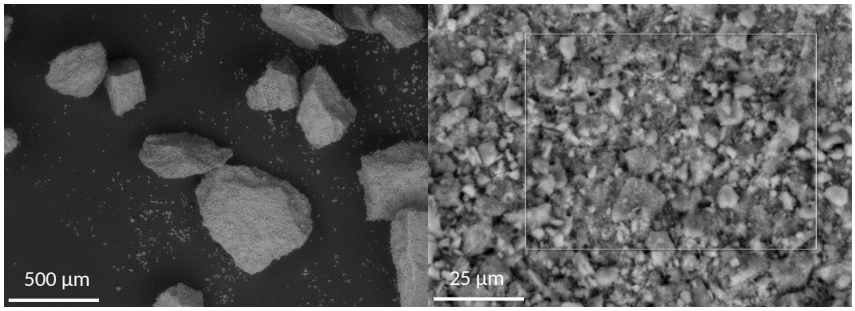

e)

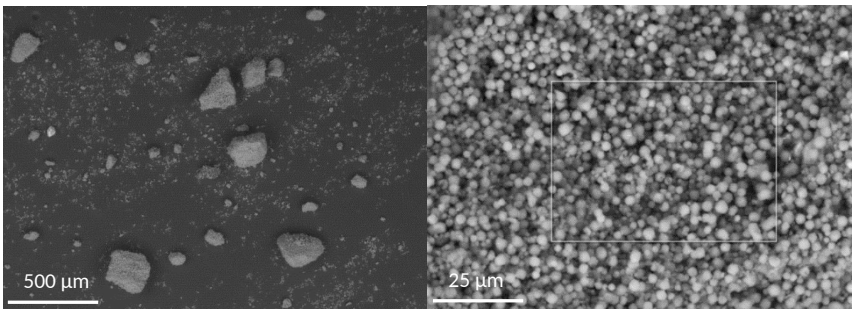

f)

Figure 7 ESEM images of a) Chem-$NaHCO_3$; b) Chem-CaO; c) Chem-Na_2CO_3-ZnO; d) Ads-Al_2O_3-1; e) Ads-Al_2O_3-2; and f) Ads-NaX chlorine removers. High magnification ESEM images show examples of rectangular areas used for the chlorine determination by EDS.

After the pyrolysis tests using mixtures of PVC, chars obtained from adsorbent containing mixtures showed a similar morphology to those of the starting materials as any changes were difficult to see due to the low proportion (5 wt.%) of char present. However, the chemical removers showed significant changes in their morphology, especially in the case of Chem-CaO, due to the formation of chlorine salts (confirmed by EDS) and particle agglomeration, and their images are presented in Figure 8 below.

a)

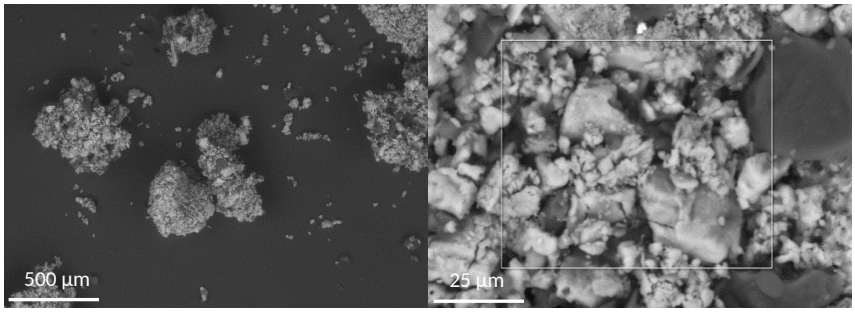

b)

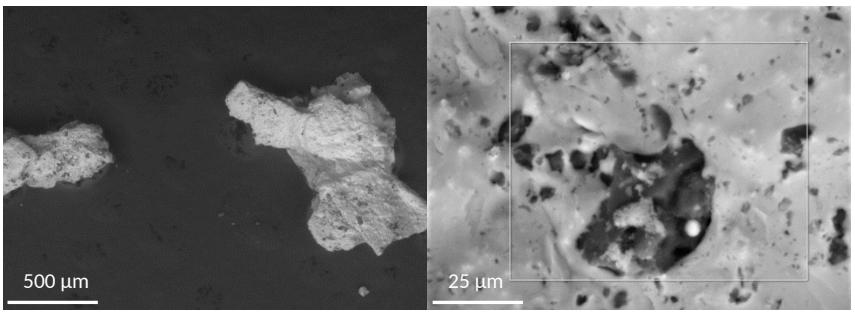

c)

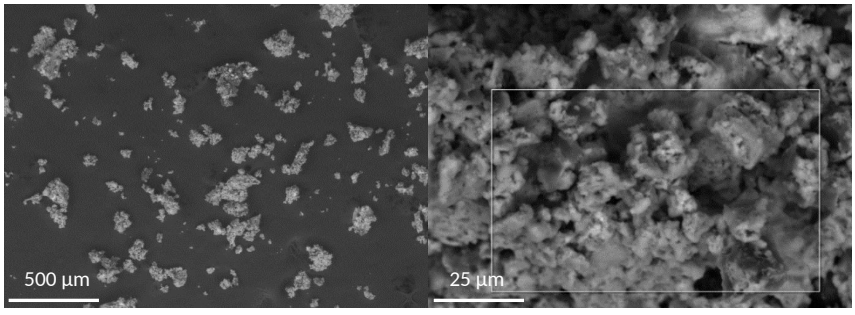

390 **Figure 8** ESEM images of a) PVC + Chem-$NaHCO_3$; b) PVC + Chem-CaO; and c) PVC +
391 Chem-Na_2CO_3-ZnO mixtures after pyrolysis in TGA at 550 ºC. High magnification ESEM
392 images show examples of rectangular areas used in the chlorine determination by EDS.
393
394 The composition of selected chars was determined by EDS to give an average estimation of
395 the chlorine content (5 large areas of each sample were analysed). This measure allows the
396 percentage of Cl retention achieved with each remover to be estimated. In Table 3 the chlorine
397 retention (wt. %) for the mixtures is given. The initial chlorine content in the starting mixtures
398 is estimated according to the manufacturer's data for pure PVC which is 56.7 wt. %. Likewise,
399 550 ºC pyrolyzed PVC showed a chlorine content of about 0.02 wt. %, which is considered in
400 the calculation of the Cl retention for the chlorine removers. In accordance with the TGA and
401 DTG curves, Chem-CaO and Chem-Na_2CO_3-ZnO showed the highest chlorine retention
402 (around 63 and 71 wt. %, respectively). The chemical removers and adsorbents showed lower
403 *onset* and ΔT in the TGA (Table 2) as the chlorine retention was higher. In addition, it should
404 be remembered that Chem-CaO still has the capacity to react with more HCl according to the
405 results of the FTIR above. In the case of adsorbents, Ads-NaX presented the poorest chlorine
406 retention, although the working conditions studied in the present work (direct contact and 550
407 ºC) are not optimal for an adsorption process. Under these conditions, the adsorbent Ads-
408 Al_2O_3-2 gave the best chlorine retention (19 wt. %). For the adsorbents, the percentile weight
409 difference measured by the TGA (see *Diff.* in Table 2) seems to be a valid indicator to follow
410 their behaviours since this parameter decreased as the Cl retention increased in the chars.
411
412 **Table 3** Chlorine retention measured by EDS of TGA chars obtained in the pyrolysis of PVC
413 at 550 ºC (from 50 ºC at 200 ºC/min) using different chlorine removers.

Sample	**Cl retention** (wt. %)

PVC	0[a]
PVC + Chem-$NaHCO_3$	49
PVC + Chem-CaO	63
PVC + Chem-Na_2CO_3-ZnO	71
PVC + Ads-Al_2O_3-1	13
PVC + Ads-Al_2O_3-2	19
PVC + Ads-NaX	8

414 a = Cl retention of 0.003 wt. %; Cl content in 550 ºC pyrolyzed char is below 0.02 wt. %.

415

416 **Conclusions**

417 The behaviour of different materials for chlorine retention in PVC pyrolysis was studied.
418 Chemicals removers (Chem-$NaHCO_3$, Chem-CaO and Chem-Na_2CO_3-ZnO) and adsorbents
419 (Ads-Al_2O_3-1, Ads-Al_2O_3-2 and Ads-NaX) were mixed with PVC (1:1; wt.) and tested in a
420 thermobalance at pyrolysis conditions (200 ºC/min heating rate from 50 to 550 ºC), and the
421 change in mass measured and resulting chars were analysed. The FTIR technique is shown as
422 a valid tool to follow the consumption of the bases present in the chemical removers and the
423 suppression of the C–Cl absorption bands of the PVC –CHCl– groups during its pyrolysis, as
424 well as the formation of some chlorine salts ($CaCl_2$ and $ZnCl_2$). This gave sufficient evidence
425 to verify the performance of this type of materials in the elimination of HCl gas. Likewise,
426 while NaCl did not absorb in the studied FTIR region, the Na_2CO_3 consumption in Chem-
427 $NaHCO_3$ and Chem-Na_2CO_3-ZnO was followed by this technique. Complementing the FTIR
428 technique, chlorine salts (NaCl, $CaCl_2$ and $ZnCl_2$) were confirmed in the corresponding chars
429 by EDS. With a detection limit of 50 ppm, the EDS technique is more effective in the
430 quantitative determination of chlorine not released during plastic pyrolysis than other methods
431 when the sample quantities are small and routinely analysed.
432 The transformation observed in the adsorbents by FTIR was minor and mainly due to the
433 thermal transformation of their constituents, although Ads-NaX showed recognizable signals

of pyrolyzed PVC. According to FTIR and CHN analysis data, the PVC pyrolysis occurs through a clear dehydrochlorination process and the formation of aromatic compounds. Chem-CaO and Chem-Na_2CO_3-ZnO had the highest chlorine retention (as the percentage that remains in the char in relation to the starting PVC) with values of 63 and 71 wt. %, respectively, although Chem-CaO still exhibited the capacity to react more HCl according to the FTIR results. Among the adsorbents, Ads-Al_2O_3-2 gave the best chlorine retention (19 wt. %) under the studied operating conditions. Likewise, the TGA data clearly showed the effect of adding a chlorine remover to the pyrolysis of PVC at 550 ºC.

Acknowledgement

The funding to support this research was awarded by Innovate UK Energy Catalyst 4. D.T. is thankful for his contract funded by this Project. Cranfield University thank the technical and material assistance received from the Recycling Technologies Ltd throughout the project and for this publication.

References

[1] E.L. Teuten, J.M. Saquing, D.R. Knappe, M.A. Barlaz, S. Jonsson, A. Björn, S.J. Rowland, R.C. Thompson, T.S. Galloway and R. Yamashita, *Philosophical Transactions of the Royal Society B: Biological Sciences*, 364, (2009) 2027.

[2] A. Marongiu, T. Faravelli, G. Bozzano, M. Dente and E. Ranzi, *Journal of Analytical and Applied Pyrolysis*, 70, (2003) 519.

[3] S.D. Anuar Sharuddin, F. Abnisa, W.M.A. Wan Daud and M.K. Aroua, *Energy Conversion and Management*, 115, (2016) 308.

[4] J. Yu, L. Sun, C. Ma, Y. Qiao and H. Yao, *Waste Management*, 48, (2016) 300.

[5] N. Lingaiah, M.A. Uddin, A. Muto, T. Imai and Y. Sakata, *Fuel*, 80, (2001) 1901.

[6] M.A. Keane, *Journal of Chemical Technology & Biotechnology*, 82, (2007) 787.

[7] K.-B. Park, S.-J. Oh, G. Begum and J.-S. Kim, *Energy*, 157, (2018) 402.

[8] H. Bockhorn, J. Hentschel, A. Hornung and U. Hornung, *Chemical Engineering Science*, 54, (1999) 3043.

[9] A. López, I. de Marco, B.M. Caballero, M.F. Laresgoiti and A. Adrados, *Fuel Processing Technology*, 92, (2011) 253.

[10] S.M. Al-Salem, A. Antelava, A. Constantinou, G. Manos and A. Dutta, *Journal of Environmental Management*, 197, (2017) 177.

[11] P. Zhao, N. Huang, J. Li and X. Cui, *Fuel Processing Technology*, 199, (2020) 106277.

[12] T. Bhaskar, R. Negoro, A. Muto and Y. Sakata, *Green Chemistry*, 8, (2006) 697.

[13] N. Sophonrat, L. Sandström, R. Svanberg, T. Han, S. Dvinskikh, C.M. Lousada and W. Yang, *Industrial & Engineering Chemistry Research*, 58, (2019) 13960.

[14] S.L. Wong, N. Ngadi, T.A.T. Abdullah and I.M. Inuwa, *Renewable and Sustainable Energy Reviews*, 50, (2015) 1167.

[15] B. Han, Y. Chen, Y. Wu, D. Hua, Z. Chen, W. Feng, M. Yang and Q. Xie, *Journal of Thermal Analysis and Calorimetry*, 115, (2014) 227.

[16] Q. Cao, G. Yuan, L. Yin, D. Chen, P. He and H. Wang, *Waste Management*, 58, (2016) 241.

[17] M. Blazsó and E. Jakab, *Journal of Analytical and Applied Pyrolysis*, 49, (1999) 125.

[18] M.F. Ali and M.N. Siddiqui, *Journal of Analytical and Applied Pyrolysis*, 74, (2005) 282.

[19] H. Kuramochi, D. Nakajima, S. Goto, K. Sugita, W. Wu and K. Kawamoto, *Fuel*, 87, (2008) 3155.

[20] A. Lopez-Urionabarrenechea, I. de Marco, B.M. Caballero, M.F. Laresgoiti and A. Adrados, *Journal of Analytical and Applied Pyrolysis*, 96, (2012) 54.

[21] M.A. Uddin, T. Bhaskar, J. Kaneko, A. Muto, Y. Sakata and T. Matsui, *Fuel*, 81, (2002) 1819.

[22] C. Tang, Y.-Z. Wang, Q. Zhou and L. Zheng, *Polymer Degradation and Stability*, 81, (2003) 89.

[23] M. Brebu, T. Bhaskar, K. Murai, A. Muto, Y. Sakata and M.A. Uddin, *Polymer Degradation and Stability*, 87, (2005) 225.

[24] D. Wang, R. Xiao, H. Zhang and G. He, *Journal of Analytical and Applied Pyrolysis*, 89, (2010) 171.

[25] N. Miskolczi, F. Ateş and N. Borsodi, *Bioresource technology*, 144, (2013) 370.

[26] C. Santella, L. Cafiero, D. De Angelis, F. La Marca, R. Tuffi and S. Vecchio Ciprioti, *Waste Management*, 54, (2016) 143.

[27] A. Veksha, A. Giannis, W.-D. Oh, V.W.C. Chang and G. Lisak, *Fuel Processing Technology*, 170, (2018) 13.

[28] B. Fekhar, L. Gombor and N. Miskolczi, *Journal of the Energy Institute*, 92, (2019) 1270.

[29] A. Lopez-Urionabarrenechea, I. de Marco, B.M. Caballero, M.F. Laresgoiti and A. Adrados, *Fuel Processing Technology*, 137, (2015) 229.

[30] M. Daoudi and J.K. Walters, *The Chemical Engineering Journal*, 47, (1991) 11.

[31] W. Wang, Z. Ye and I. Bjerle, *Fuel*, 75, (1996) 207.

[32] W. Kaminsky and J.-S. Kim, *Journal of Analytical and Applied Pyrolysis*, 51, (1999) 127.

[33] M. Li, H. Shaw and C.-L. Yang, *Industrial & Engineering Chemistry Research*, 39, (2000) 1898.

[34] Y. Masuda, T. Uda, O. Terakado and M. Hirasawa, *Journal of Analytical and Applied Pyrolysis*, 77, (2006) 159.

[35] K.-Y. Chiang, J.-C. Jih and K.-L. Lin, *Journal of Hazardous Materials*, 157, (2008) 170.

[36] T. Kameda, N. Uchiyama, K.-S. Park, G. Grause and T. Yoshioka, *Chemosphere*, 73, (2008) 844.

[37] H.M. Zhu, X.G. Jiang, J.H. Yan, Y. Chi and K.F. Cen, *Journal of Analytical and Applied Pyrolysis*, 82, (2008) 1.

[38] C.-S. Chyang, Y.-L. Han and Z.-C. Zhong, *Energy & Fuels*, 23, (2009) 3948.

[39] C.-S. Chyang, Y.-L. Han, L.-W. Wu, H.-P. Wan, H.-T. Lee and Y.-H. Chang, *Waste Management*, 30, (2010) 1334.

[40] Z. Sun, F.-C. Yu, F. Li, S. Li and L.-S. Fan, *Industrial & Engineering Chemistry Research*, 50, (2011) 6034.

[41] S. Kumagai, I. Hasegawa, G. Grause, T. Kameda and T. Yoshioka, *Journal of Analytical and Applied Pyrolysis*, 113, (2015) 584.

[42] S. Pachitsas, L. Skaarup Jensen, S. Wedel, J. Boll Illerup and K. Dam-Johansen, *Journal of Environmental Chemical Engineering*, 7, (2019) 102869.

[43] M. Al-Harahsheh, A. Al-Otoom, L. Al-Makhadmah, I.E. Hamilton, S. Kingman, S. Al-Asheh and M. Hararah, *Journal of Hazardous Materials*, 299, (2015) 425.

[44] J. Zhou, B. Gui, Y. Qiao, J. Zhang, W. Wang, H. Yao, Y. Yu and M. Xu, *Fuel*, 166, (2016) 526.

[45] T. Yoshioka, T. Kameda, S. Imai and A. Okuwaki, *Polymer Degradation and Stability*, 93, (2008) 1138.

[46] R.R. Stromberg, S. Straus and B.G. Achhammer, *J. Res. Natl. Bur. Stand.*, 60, (1958) 147.

[47] M. Theodorou and B. Jasse, *Journal of Polymer Science: Polymer Physics Edition*, 21, (1983) 2263.

[48] E. Pretsch, P. Bühlmann and M. Badertscher, *Structure Determination of Organic Compounds. Tables of Spectral Data*, Springer-Verlag Berlin Heidelberg, 2009, p. XV.

[49] J. Wu, T. Chen, X. Luo, D. Han, Z. Wang and J. Wu, *Waste Management*, 34, (2014) 676.

[50] T. Li, P. Zhao, M. Lei and Z. Li, *Applied Sciences*, 7, (2017) 256.

[51] D.J. Fray, *Plastics, Rubber and Composites*, 28, (1999) 327.

[52] K. Sharma, A. Vyas and S.K. Singh, *Catalyst*, 1, (2015) 200.

[53] X. Ren, E. Rokni, Y. Liu and Y.A. Levendis, *Journal of Energy Engineering*, 144, (2018) 04018045.

[54] T. Baird, J.R. Fryer and B. Grant, *Carbon*, 12, (1974) 591.

[55] S. Hosseini, A. Niaei and S. D., *Open J. Phys. Chem.*, 1, (2011) 23.

[56] S. Joshi, S. Kalyanasundaram and V. Balasubramanian, *Applied Spectroscopy*, 67, (2013) 841.

[57] M. Kooti and A. Naghdi Sedeh, *Journal of Chemistry*, 2013, (2013) 4.

[58] T.N. Tran, T.V. Anh Pham, M.L. Phung Le, T.P. Thoa Nguyen and V.M. Tran, *Advances in Natural Sciences: Nanoscience and Nanotechnology*, 4, (2013) 045007.

[59] M.Z.M. Noor, N.A. Sollahunddin and S. Irawan, *Proceedings*, 2, (2018) 1273.

[60] P. Raizada, P. Shandilya, P. Singh and P. Thakur, *Journal of Taibah University for Science*, 11, (2017) 689.

[61] T. Kalaycı and B. Bardakçı, *Protection of Metals and Physical Chemistry of Surfaces*, 50, (2014) 709.

[62] W. Rongchapo, C. Keawkumay, N. Osakoo, K. Deekamwong, N. Chanlek, S. Prayoonpokarach and J. Wittayakun, *Adsorption Science & Technology*, 36, (2018) 684.

[63] F. Iskandar, N.A. Zen, T.R. Mayangsari, A.H. Aimon and A.A. Pramana, *Materials Research Express*, 6, (2019) 045510.

[64] E.K. Tiburu, M. Mutocheluh, P.K. Arthur, P.W. Narkwa, A.A. Salifu, M.A. Agyei, R. Yeboah, H.N.A. Fleischer, J. Zhuang and G. Awandare, *Journal of Biomaterials and Tissue Engineering*, 7, (2017) 544.

[65] O. Yasar-Inceoglu, T. Lopez, E. Farshihagro and L. Mangolini, *Nanotechnology*, 23, (2012) 255604.

[66] J.W. Elam, C.E. Nelson, M.A. Tolbert and S.M. George, *Surface Science*, 450, (2000) 64.

[67] R. Sharma, T. Segato, M.-P. Delplancke, H. Terryn, G.V. Baron, J.F.M. Denayer and J. Cousin-Saint-Remi, *Chemical Engineering Journal*, 381, (2020) 122512.

[68] I.É. Gel'ms, V.I. Yuzefovich and R.N. Yudinson, *Chemistry and Technology of Fuels and Oils*, 3, (1967) 631.

Hydrochloric acid removal from the thermogravimetric pyrolysis of PVC

Torres, Daniel

2020-05-04

Torres D, Jiang Y, Sanchez Monsalve DA, Leeke GA. (2020) Hydrochloric acid removal from the thermogravimetric pyrolysis of PVC. Journal of Analytical and Applied Pyrolysis, Volume 149, August 2020, Article number 104831

https://doi.org/10.1016/j.jaap.2020.104831